Anomalous magnetic noise in an imperfectly flat landscape in the topological magnet $Dy_2Ti_2O_7$

Anjana M. Samarakoon[a,b], S. A. Grigera[c,1], D. Alan Tennant[a,b,d], Alexander Kirste[e], Bastian Klemke[f], Peter Strehlow[e], Michael Meissner[f], Jonathan N. Hallén[g,h], Ludovic Jaubert[i], Claudio Castelnovo[g], and Roderich Moessner[h]

[a]Neutron Scattering Division, Oak Ridge National Laboratory, Oak Ridge, TN 37831; [b]Shull Wollan Center—A Joint Institute for Neutron Sciences, Oak Ridge National Laboratory, Oak Ridge, TN 37831; [c]Instituto de Física de Líquidos y Sistemas Biológicos, Universidad Nacional de La Plata - Consejo Nacional de Investigaciones Científicas y Técnicas, La Plata, Argentina; [d]Quantum Science Center, Oak Ridge National Laboratory, Oak Ridge, TN 37831; [e]Physikalisch-Technische Bundesanstalt, 10587 Berlin, Germany; [f]Helmholtz-Zentrum Berlin für Materialien und Energie, D-14109 Berlin, Germany; [g]Theory of Condensed Matter Group, Cavendish Laboratory, University of Cambridge, Cambridge CB3 0HE, United Kingdom; [h]Max Planck Institute for the Physics of Complex Systems, 01187 Dresden, Germany; and [i]CNRS, Laboratoire Ondes et Matière d'Aquitaine, UMR 5798, Université de Bordeaux, 33400 Talence, France

Noise generated by motion of charge and spin provides a unique window into materials at the atomic scale. From temperature of resistors to electrons breaking into fractional quasiparticles, "listening" to the noise spectrum is a powerful way to decode underlying dynamics. Here, we use ultrasensitive superconducting quantum interference device (SQUIDs) to probe the puzzling noise in a frustrated magnet, the spin-ice compound $Dy_2Ti_2O_7$ (DTO), revealing cooperative and memory effects. DTO is a topological magnet in three dimensions—characterized by emergent magnetostatics and telltale fractionalized magnetic monopole quasiparticles—whose real-time dynamical properties have been an enigma from the very beginning. We show that DTO exhibits highly anomalous noise spectra, differing significantly from the expected Brownian noise of monopole random walks, in three qualitatively different regimes: equilibrium spin ice, a "frozen" regime extending to ultralow temperatures, and a high-temperature "anomalous" paramagnet. We present several distinct mechanisms that give rise to varied colored noise spectra. In addition, we identify the structure of the local spin-flip dynamics as a crucial ingredient for any modeling. Thus, the dynamics of spin ice reflects the interplay of local dynamics with emergent topological degrees of freedom and a frustration-generated imperfectly flat energy landscape, and as such, it points to intriguing cooperative and memory effects for a broad class of magnetic materials.

frustrated magnets | constrained dynamics | spin ice | noise measurements | glass physics

S pin-ice materials are a paradigmatic example of three-dimensional topological behavior (1–3). Their prominence as a model system is supported by a remarkable level of quantitative agreement between experiment and relatively simple theoretical models, which has allowed for detailed understanding of the mechanisms underpinning their exotic equilibrium behavior in a way that is rare in strongly interacting many-body physics.

$Dy_2Ti_2O_7$ (DTO) is a canonical classical spin ice (2). The configurations satisfying the ice rules form an effectively degenerate set of ground states, on top of which magnetic monopole defects are the gapped elementary low-energy excitations (4) (Fig. 1). At low temperatures, this regime is topological, in that it is elegantly described by the Coulomb phase of an emergent magnetostatics. Its spin dynamics, dominantly generated by the motion of these monopoles, slows down as these become increasingly sparse upon cooling.

Given the importance of spin models to the understanding of cooperative phases and transitions, it is all the more remarkable how enigmatic the dynamics of spin-ice systems remains to date. Different experiments in DTO (5–8) indicate a rapid slowdown of the dynamics upon lowering temperature. On a qualitative level, this can be understood by combining the well-established classical model Hamiltonian with a single spin-flip dynamics

appropriate for Ising systems (9–11). Under the assumption of a unique and temperature-independent spin-flip timescale (denoted by τ_u; e.g., due to single-ion quantum spin tunneling) (12), a Lorentzian form for the magnetic susceptibility is predicted (9). To leading order, this has a characteristic magnetic relaxation timescale obeying an Arrhenius law at low temperatures inversely proportional to the monopole density, which is indeed activated (10). This theory, however, fails to account for the non-Lorentzian shape of the curve while quantitatively strongly underestimating the actual growth of the timescale (see Fig. 3 for a review of the data in the literature) as well as failing to capture the nature of the irreversibility appearing around $T_{irr} \approx 0.6$ K.

Here, we address the origin of the anomalous cooperative dynamics and whether it is intrinsic to spin ice. Attempts to explain such discrepancies resulted in models invoking finite-sized effects, open boundary conditions, a temperature-dependent timescale, and chemical substitution disorder (7, 13–17). Recently, an intriguing analogy between spin-ice phenomenology and generation/recombination noise in semiconductors was drawn based on high-temperature superconducting quantum interference device (SQUIDs) measurements (18). In general, the anomalous behavior of spin-ice materials is often related to the physics of supercooled liquids and a possible avoided phase transition (6, 19–21). However, it is fair to say that a satisfactory understanding is still very much missing.

We report noninvasive SQUID noise measurements with unprecedented sensitivity and access to low temperatures

Significance

Ultrasensitive low-temperature magnetic noise experiments on a network of atomic spins reveal how anomalous "glassy" dynamics can arise in a topological magnet, even in the absence of disorder. The results uncover an interplay of local dynamics with emergent topological degrees of freedom and a frustration-generated imperfectly flat energy landscape, and as such, they point to intriguing cooperative and memory effects for a broad class of magnetic materials.
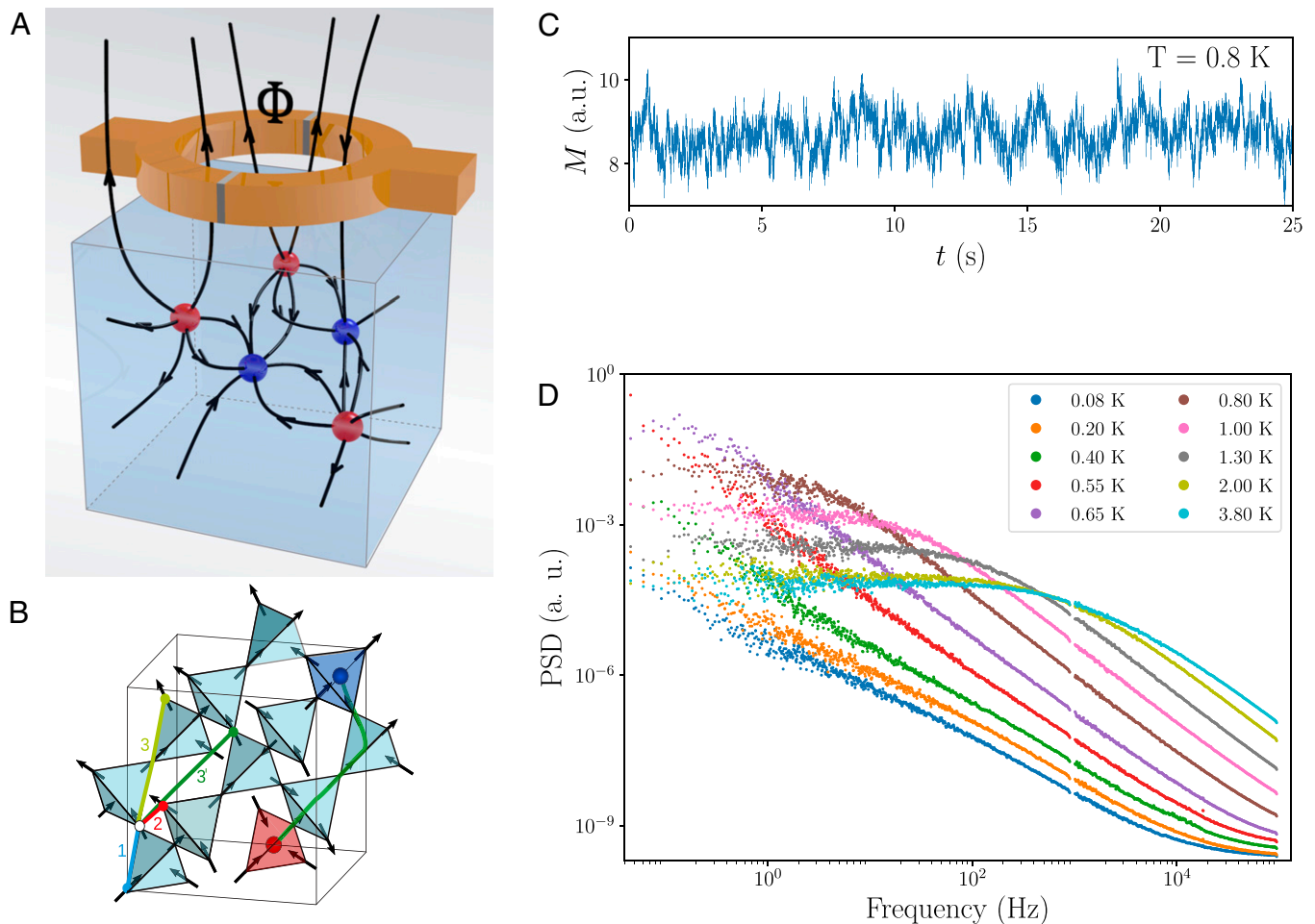
PHYSICS

Fig. 1. Magnetic structure, monopole hopping, and anomalous noise measurements in DTO. (*A*) Schematic view of the experiment. Monopoles, depicted in red and blue, move, and the resulting change in magnetic flux at the surface is detected by a SQUID. (*B*) The spins in DTO are located on a pyrochlore lattice. The magnetic interaction pathways are shown in color. These together with long-range dipolar interactions constrain the spin configurations to follow two-in, two-out ice rules. Breaking the ice rules results in the creation of a monopole antimonopole pair, which can separate, leaving behind a Dirac string (green). Monopoles are constrained by the other spins to travel over a restricted manifold. (*C*) Experimental magnetic noise in the time domain. (*D*) The PSD signal for a selection of temperatures covering the full temperature range. The displayed temperatures are given. Each curve is composed of two datasets with different sampling rates (and hence, different frequency windows), causing the gap in the PSD around 10^3 Hz.

(Fig. 1), enlarging the experimental data for the dynamics across a broad range of temperatures and frequencies. We also present a detailed set of Monte Carlo simulations investigating different model families for spin-ice systems. We show intrinsic anomalous dynamics in spin ice originating from memory effects of monopole motion in the imperfectly flat energy landscape provided by the ice configurations of DTO, but we also appear to observe important contributions from more complex spin-flip dynamics.

SQUID Noise Measurements

We use an ultrasensitive SQUID microsusceptometer to measure in a direct way magnetic noise across a broad temperature window from 0.08 to 4 K. The experiment was set up in an adiabatic demagnetization refrigerator at the Physikalisch-Technische Bundesanstalt, Berlin. The SQUID-based setup allows measurement sensitivities of 10^{-15} T in the magnetic field due to the sample (details are in *SI Appendix*, section 1).

A high-quality single crystal of DTO was mounted on top of the SQUID sensor, and the magnetic flux was recorded as a function of time, spanning the frequency range ν from 0.01 to 10^5 Hz. The measurements were started at base temperature and undertaken over a period of 24 h while the sample slowly warmed.

The single crystal was isotopically enriched to result in zero nuclear moment to ensure that the magnetic signal emanates exclusively from the electronic moments.

Results

Fig. 1*D* summarizes the results, displaying the noise power spectral density (PSD) from 0.08 to 3.8 K. Two datasets were combined to improve the statistics. The experimental noise measurements cover about seven orders of magnitude in frequency and nine orders of magnitude in noise power, demonstrating the sensitivity and dynamical range of the apparatus.

At high temperature, the curves exhibit a plateau at low frequency and a decay at high frequency. These features are separated by a knee, which moves to lower frequencies as the temperature is lowered until it is eventually squeezed out of the measurement window, while the total noise power also decreases. We distinguish three different temperature regimes. The high-temperature paramagnetic regime crosses over to the spin-ice regime around $T \approx 1$ K as the spin-ice correlations gradually develop. As the temperature is lowered below $T_{irr} \approx 0.6$ K, the irreversibility temperature of magnetization measurements, the system enters a nonequilibrium regime characterized by extremely long magnetic relaxation times.
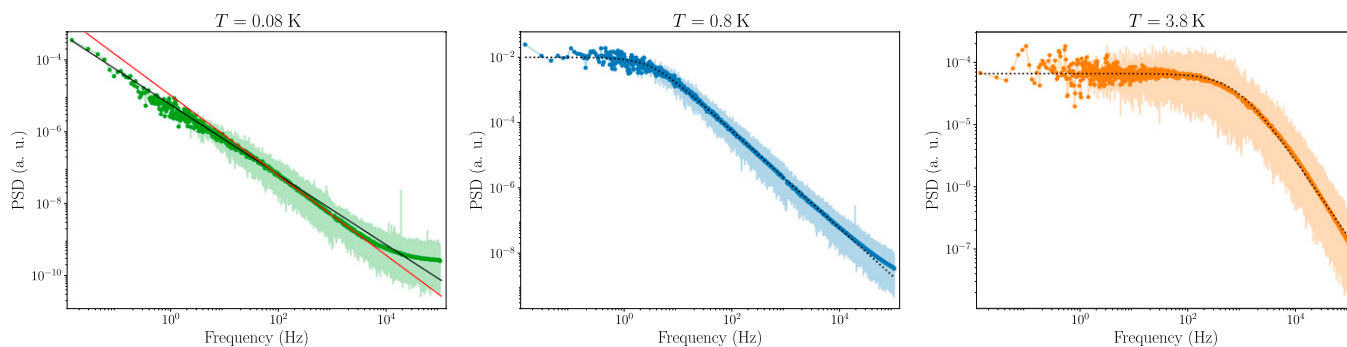
Fig. 2. The raw (transparent lines) and window-averaged (opaque points) PSD signals at three temperatures. (*Left*) At low temperatures, the PSD acquires an S shape suggestive of (at least) two distinct contributions at low and high frequencies. The black and red lines are guides to the eye and have approximate slopes of 0.98 and 1.12, respectively. (*Center*) In the range between 750 mK and 1.5 K, a Cole–Cole form (dotted black line) fits the data well. (*Right*) At higher temperatures ($\gtrsim$1.5 K), the knee between the plateau and scaling behavior broadens. The high-frequency scaling regime is less clearly established, and fitting for the exponent becomes more uncertain. The fitted values of the exponent α and the timescale τ are shown in Fig. 3.

We start by focusing on the spin-ice regime, which is of central interest to this study. Fig. 2, *Center* shows the frequency dependence of the noise power at $T = 0.8$ K alongside a fit to a Cole–Cole form:

$$S_{\text{CC}}(\nu) = \frac{A}{1 + (2\pi\nu\tau)^{\alpha}} \,. \qquad [1]$$

The fit works very well over the full frequency range; the main deviation is at the lowest frequencies, where the experimental data exhibit a weak rise rather than a perfect plateau. Two features stand out in the fit. First, it covers a region of more than six orders of magnitude along both axes (i.e., frequency and noise power). Second, it exhibits an anomalous exponent, $\alpha \approx 1.5$, as opposed to the $\alpha = 2$ of a simple Lorentzian. More details on the data analysis and fitting procedure are given in *SI Appendix*.

Indeed, this is our first central experimental result; spin ice is well known to be fully equilibrated at these temperatures, as hysteresis, history dependence, and other signatures of out-of-equilibrium behavior only set in around T_{irr}. Nonetheless, its noise spectrum exhibits a form otherwise familiar from the study of glasses and supercooled liquids.

Turning toward the paramagnetic regime at higher temperatures (Fig. 2, *Right*), the shape of the curve evolves slowly, with the knee softening somewhat. The dynamical range accessible in noise power decreases with the strength of the overall signal, and the uncertainty in the fitting parameters grows (discussion is in *SI Appendix*).

Third, in the nonequilibrium low-temperature regime, the curve becomes more complex entirely. Furthermore, the absence of a plateau makes the fit to Eq. **1** somewhat poorly constrained. However, even in the accessible data window, it is apparent that there are (at least) two different portions with different anomalous slopes at intermediate and high frequency, with a possible further upturn (which however, may be caused by the sensor noise), endowing the curve with an "S" shape (Fig. 2, *Left*). A simple fitting form like the one used in equilibrium, therefore, no longer suffices. Additionally, the system is out of equilibrium, and the details of the curve can depend on the preparation history of the measurement.

If one takes the parameters obtained from the equilibrium regimes at face value, two things are notable. First, the temperature dependence of the characteristic timescales $\tau(T)$ (purple circles in Fig. 3, *Lower*) is close to those obtained previously by means of alternating current susceptibility measurements (19), specific heat (8), and high-temperature SQUID noise experiments (18) on single crystals. Second, the power α (Fig. 3, *Upper*) does not get close to two (Lorentzian behavior) at any temperature. Indeed, it seems to become even smaller (i.e., more anomalous) with increasing temperature.

Modeling

The highly non-Lorentzian relaxation is perhaps the most striking aspect of the dynamics in the spin-ice regime, where we know the system equilibrates and does not exhibit any glassy behavior. The fact that it becomes less Lorentzian as the temperature is increased, where spin ice increasingly resembles a conventional paramagnet, is a separate surprise.

In order to determine the possible sources of this behavior, we have conducted extensive simulations of the dynamics of spin ice. To do so, we have adopted the τ_u-dynamics introduced above (9–11). This is a stochastic model of incoherent dynamics, which only has the single timescale τ_u as the input parameter. The timescale can be thought of as an effective (inverse) spin-flip attempt rate
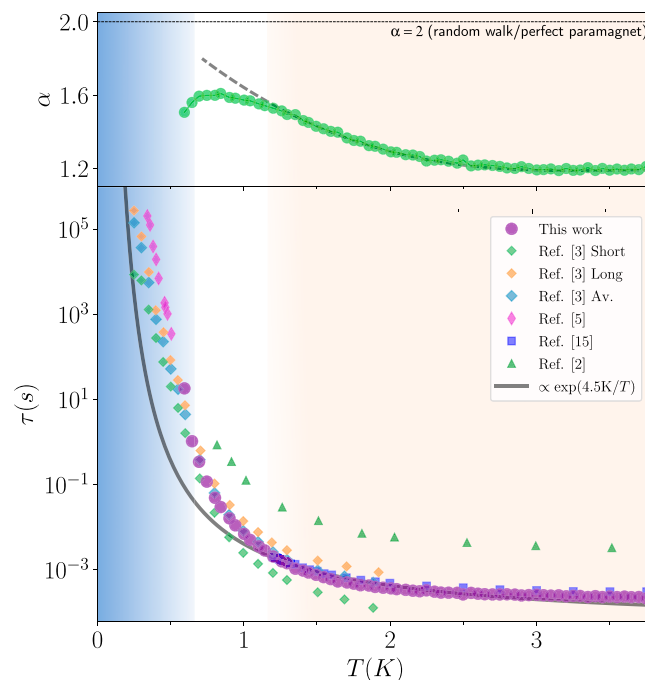

Fig. 3. Anomalous exponent (*Upper*) and characteristic relaxation timescale τ (*Lower*) extracted from Cole–Cole fits to the experimentally measured PSD. The characteristic time is compared with values found in the literature using various techniques and with an Arrhenius law. The shaded background indicates the three different temperature regimes: paramagnetic (orange), spin ice (white), and nonequilibrium (blue). The dashed line in *Upper* is an extrapolation of the high-temperature behavior of α into the spin-ice regime.
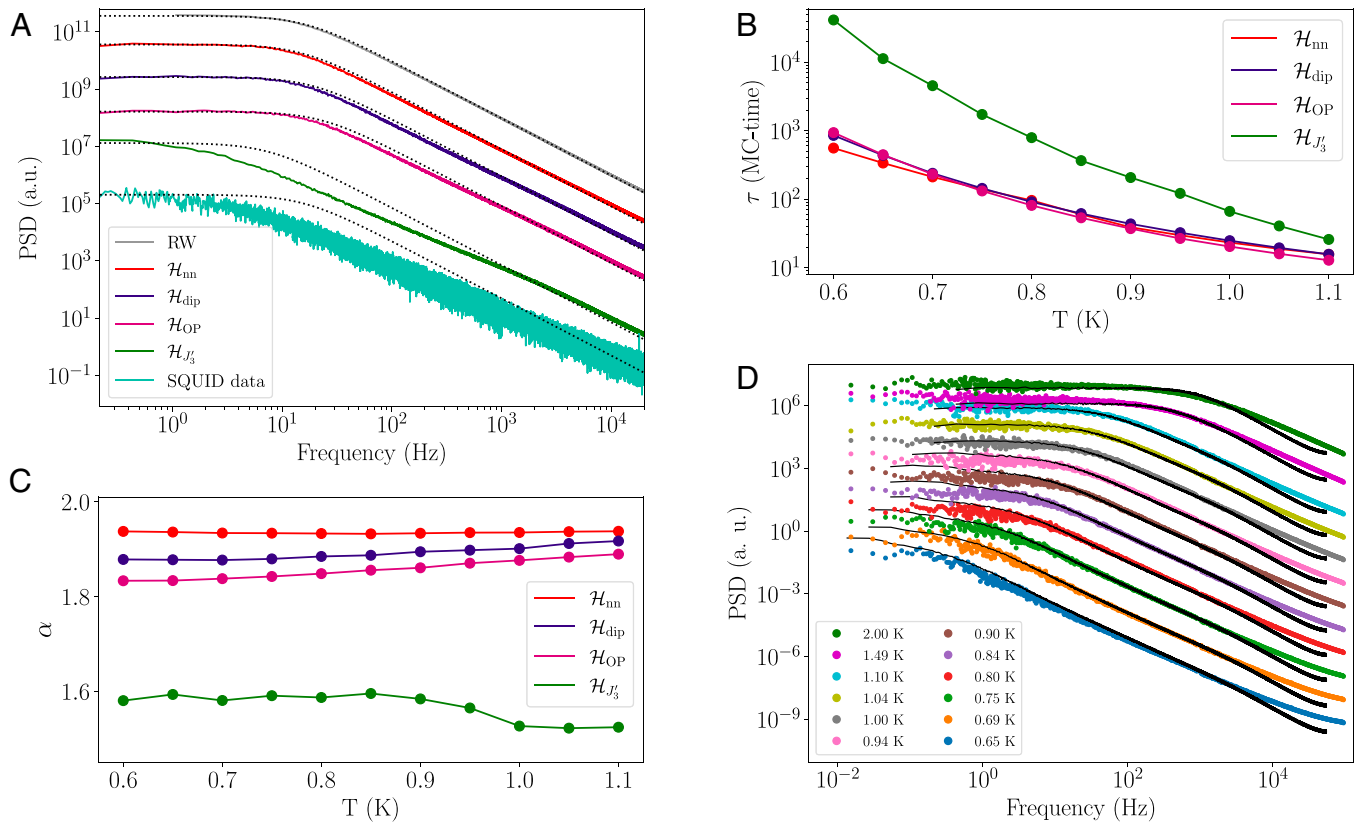
PHYSICS

Fig. 4. (*A*) PSDs of (from top to bottom) a random walk (RW) on a diamond lattice; Monte Carlo (MC) simulations of the four spin-ice Hamiltonians $\mathcal{H}_{nn}$, $\mathcal{H}_{dip}$, $\mathcal{H}_{OP}$, and $\mathcal{H}_{J_3'}$; and experimental SQUID data at $T = 0.8$ K (shifted vertically for clarity). The spin-ice Monte Carlo simulations were performed on a system of size $L = 10$ with periodic boundary conditions and a 16-spin cubic unit cell. The dotted black curves are fits of the form $A/(1 + \tau^2\nu^2)$, showing how the models display more anomalous decay as we move down the plot. (*B*) Characteristic relaxation timescale τ and (*C*) anomalous exponent for the model Hamiltonians $\mathcal{H}_{nn}$, $\mathcal{H}_{dip}$, $\mathcal{H}_{OP}$, and $\mathcal{H}_{J_3'}$. Parameters are extracted from Cole–Cole fits to Monte Carlo data (*SI Appendix* has details). (*D*) Comparison of the experimental curves (symbols) and Monte Carlo simulations (black lines) for the Hamiltonian $\mathcal{H}_{J_3'}$. Temperatures from top to bottom are listed; the PSD curves are shifted vertically for clarity.

that an isolated moment in spin ice would have. The actually observed spin-flip rate then also takes into account the exchange field due to its interaction partners via an acceptance probability $p = \min\{1, \exp(-\beta\,\Delta E)\}$ given by standard Metropolis dynamics at temperature T for an energy difference ΔE between initial and final states. An appraisal of this assumption a posteriori will form an important part of our discussion.

We next present our analysis of such dynamics in a physically motivated set of spin-ice models. These are based on the current best effective DTO Hamiltonian $\mathcal{H}_{OP}$ (22). $\mathcal{H}_{OP}$ involves strong nearest neighbor (nn) and dipolar interactions with weaker second and third neighbor interactions and reproduces equilibrium as well as irreversible behavior. Our additional models are the simple nn spin-ice model, $\mathcal{H}_{nn}$; extension to include dipolar coupling, $\mathcal{H}_{dip}$; and further addition of the third neighbor interaction, $\mathcal{H}_{J_3'}$ (*SI Appendix* has detailed definitions). We finally contrast these to an unrestricted random walk process for the monopoles yielding a straightforward Lorentzian behavior. (We note that $\mathcal{H}_{dip}$ and $\mathcal{H}_{OP}$ undergo thermodynamic ordering transitions at $T \approx 0.18$ K.)

We first compare the behavior of these models with the experiment in the equilibrated spin-ice regime ($T = 0.8$ K) (Fig. 4). It is immediately apparent that the random walk produces essentially perfect Lorentzian behavior, with $\mathcal{H}_{nn}$ likewise only deviating by an almost imperceptible amount matching theoretical expectations. Surprisingly, anomalies become apparent in $\mathcal{H}_{dip}$ and even more so for $\mathcal{H}_{OP}$. α is in fact quite tunable, and it drifts considerably as the strength of the farther neighbor interaction

J_3' is varied (*SI Appendix*). For $\mathcal{H}_{J_3'}$, the best match to the data ($J_3' = 0.4$ K) results in strong anomalous behavior (Fig. 4 *C* and *D*).

Crucially, we have thus identified a group of quite simple, disorder-free model Hamiltonians that exhibit variably anomalous noise, implying a broad distribution of timescales, even though the microscopic spin dynamics is parameterized by a single rate.

We next address the high-temperature regime only briefly as there is a fine recent pioneering study devoted to this, which studied the noise in spin ice down to a temperature $T = 1.2$ K (18). In this regime, the narrow range in frequency can artificially lower the value of α (*SI Appendix*, sections 4 and 6). Be the uncertainty in the fitting procedure as it may, the central finding is that experiments depart significantly from a Lorentzian behavior at high temperatures, whereas Monte Carlo simulations do not.

The root of this departure must, therefore, lie in features not included in the model with τ_u-dynamics. As argued below, it would seem rather natural that more complex spin-flip behavior, rather than a purely cooperative effect of the spins, plays a role here, with an interplay of phonons, higher crystal field levels, and a broadening distribution of local environments standing out as likely culprits.

We finally turn to the low-temperature regime, where spin ice falls out of equilibrium at $T_{irr} \approx 0.6$ K. This regime has been extensively studied using neutron scattering and susceptibility measurements (5, 6, 13, 23, 24) as well as a number of time-dependent protocols for, for example, the magnetization, aimed

at eliciting details of the nonequilibrium behavior (15, 25–28). Although the dynamical origin of this freezing is still not very well understood, the irreversibility is captured by $\mathcal{H}_{OP}$ (22). Thanks to the wide temperature and frequency range, our data provide some insights. First, as expected, the knee terminating the low-frequency plateau moves toward low frequencies upon cooling. This simply reflects the well-known slowing down of the dynamics in spin ice (5) as the monopoles become sparser (9). The latter is also evident in the noticeable decrease of the total noise power as the temperature is lowered below T_{irr}.

Additional structure emerges in the noise spectrum as can occur when there are two (parametrically) distinct timescales present. Most simply, two superposed Lorentzians, with the slow one corresponding to a larger signal, would yield an S-shape profile as observed. It is tempting to speculate that here we have, on the one hand, the relatively fast motion of monopoles trapped in their individual surroundings where, however, the confined paths cannot lead to a large change of the magnetization and on the other hand, rare longer-distance excursions of monopoles toward, for example, another local trap. Naturally, one can extend such an argument to a phenomenology based on an ensemble of Lorentzians with a distribution of characteristic timescales chosen to fit the experiment (9).

Discussion

Taken together, the theoretical modeling situation can be perhaps succinctly summarized as follows. An entirely memory-free, unconstrained random motion of monopoles with a single temperature-independent flipping rate, τ_u, yields the normal (Lorentzian) power $\alpha = 2$. This, however, is modified by two mechanisms originating in local spin-flip and cooperative effects, with opposite predominance at high and low temperatures.

The cooperative effects have several origins. First, the Dirac strings lead to anticorrelations in the monopole hops; their effect on α, however, turns out to be tiny. Next are the long-range dipolar interactions, which can be meaningfully broken down (29) into its ("projectively equivalent") Coulomb component, which preserves a flat energy landscape for the ground states, and quadrupolar and higher-order corrections, which do not. The contribution due to the former is also tiny, whereas the latter leads to a visibly anomalous behavior, albeit still far from that observed experimentally. $\mathcal{H}_{OP}$ and $\mathcal{H}_{J_3'}$ then include additional features in the form of farther neighbor interactions, yielding yet more anomalous behavior.

Therefore, frustration yields an approximately flat energy landscape, in which the spin-ice regime with its monopoles as topological defects arises. Due to this flatness, the monopoles remain mobile, and their motion produces a noise signal over a broad temperature range. Thanks to our sensitive low-T measurements, this signal remains detectable even in the regime where the monopoles become sparse.

In a featureless energy landscape, the monopole motion is well approximated by a featureless "Lorentzian" walk, $\alpha \approx 2$. It is when the energy landscape becomes complex in the presence of perturbations away from the ideal spin-ice model that the anomalous behavior sets in. Interestingly, our results suggest that entropic and energetic contributions that retain the degeneracy between the ice states and hence, do not lead to ordering are also least (if at all) effective at producing anomalous behavior. By contrast, the progressive increase in anomalous behavior suggests that the leading effect on the noise is due to interactions that ultimately cause spin ice to order, and it is evident even far above the corresponding ordering temperature—the "opposite" of supercooling, as it were.

The combination of frustration-induced flatness and perturbation-induced complexity of the landscape we believe should be a general conceptual framework for understanding disordered states and anomalous noise in topological magnets.

Indeed, similar considerations appear to be at play in diverse systems (30–34), including artificial nanomagnetic arrays, as it was recently demonstrated in ref. 35.

Returning to the actual material, neither $\mathcal{H}_{OP}$ nor $\mathcal{H}_{J_3'}$ can accurately describe the thermodynamics and dynamical behavior of DTO. $\mathcal{H}_{OP}$ has its origin in a detailed machine learning–based analysis of equilibrium neutron scattering, susceptibility, and specific heat data and can accurately reproduce a number of thermodynamic properties of DTO beyond those used for its training. It qualitatively shows the expected anomalous noise behavior but quantitatively falls short of the mark. Variations on its parameters to better fit the noise pattern result in $\mathcal{H}_{J_3'}$ at the expense of the correct thermodynamical description of the material. Furthermore, none of the simulations capture the high-temperature experimental behavior that becomes progressively more, rather than less, anomalous as temperature is increased. This is surprising from the perspective of the τ_u-model, whose single spin-flip dynamics (appropriate for a paramagnet) yields a simple Lorentzian at high temperatures.

Let us revisit the central dynamical assumption of a single temperature-independent single–spin flipping rate encoded by τ_u. The underlying spin-flip process involves the flipping of a large spin with a considerable Ising barrier in the presence of a "bath" of phonons with temperature-dependent occupancies and structure in its density of states (12, 36). The Ising barrier itself microscopically derives from a complex crystal field–level scheme, which in turn, allows various flipping paths involving activation over or tunnelling through the barrier. Their respective rates will in general depend on temperature, allowing a complex temperature dependence of the resulting net rate. In addition, these flip rates depend on the local spin configurations (e.g., via the local distribution of transverse fields providing effective matrix elements between the crystal field levels) and in fact, may involve several spins flipping in a correlated fashion. As the temperature rises, more flipping processes contribute, and the distribution of local environments broadens both spatially and temporally, so that one would expect increasing complexity of the resulting dynamics.

Turning to the signatures of complex spin-flip dynamics in detail, we note that already at low temperature, there is a divergence of the dynamical timescale $\tau(T)$ extracted from experiment, which is in excess of the cost of an isolated monopole, generally expected to set the single spin-flip timescale (9). The simplest reason for such a discrepancy would be an autonomous Arrhenius law of the effective spin-flip attempt rate, rather than a cooperative effect.

In turn, the anomalous behavior of α in DTO (Fig. 3) can be understood in terms of two countervailing mechanisms; as the temperature is lowered starting in the paramagnetic regime, the anomaly with its origin in the spin-flip dynamics decreases with the corresponding increase in α, which should eventually reach $\alpha = 2$ (dashed line in Fig. 3) were it not counteracted by the second effect, the gradual onset of cooperative effects within the spin model. Together, these opposing tendencies lead to a leveling off of α before in the frozen phase, an analysis in terms of a single exponent no longer accounts for the complexity of the anomalous behavior entirely.

In this picture, the size of the anomaly has two sizeable contributions at 0.8 K: a spin flip and a cooperative one. Absent a detailed analysis of the former, their respective sizes are not available quantitatively. An initial starting assumption suggested by the data is for both contributions to be roughly of equal size in this regime. In that case, the size of the anomaly observed in simulations of $\mathcal{H}_{OP}$ would actually be consistent with the experimental results.

This scenario has the attraction that it fits all the thermodynamic experimental data—heat capacity, neutron scattering, noise, magnetic susceptibility, magnetization, etc.—within the purview of $\mathcal{H}_{OP}$, but it still requires future work to obtain a

Samarakoon et al.
Anomalous magnetic noise in an imperfectly flat landscape in the topological magnet Dy2Ti2O7

PNAS | 5 of 6
https://doi.org/10.1073/pnas.2117453119

detailed description of the single-ion dynamics needed to complete the numerical modeling of the dynamic properties of these systems.

Independently of this sharpening of our understanding of the modeling of the DTO spin-ice material, a central theoretical insight is that the anomalous behavior, encoded by the downturn of α, can arise cooperatively—but not entirely straightforwardly. In particular, our simulations demonstrate that it is a phenomenon due to corrections beyond the ideal Coulomb gas description. Neither Dirac strings nor Coulomb interactions between monopoles produce a sizeable anomaly; rather, it is induced by farther range (beyond nn) interactions, which endow the energy landscape for monopole motion with additional structure. The resulting behavior resembles a supercooled liquid, but it can evidently happen above any thermodynamic transition temperature.

From a more conceptual perspective, a finite-frequency response, such as the one probed here, will inevitably be sensitive to a combination of universal behavior—such as phase ordering—and nonuniversal microscopic details. Both turn out to be very interesting in spin-ice materials.

Conclusion

Our ultrasensitive SQUID study reveals many facets of anomalous dynamics in DTO. Frustration yields an unusual topological magnetic state supporting magnetic monopole excitations. While the simplest nn and dipolar spin-ice models show (close to) Lorentzian behavior, experiments as well as more realistic model Hamiltonians show evidence of intrinsic anomalous dynamics. We identify a family of models that shows how perturbations that generate a complex energy landscape result in memory effects. Although supercooled like, this robustly non-Lorentzian behavior can occur as a precursor far above the actual ordering. Further, compelling evidence for complex spin-flip dynamics contributing to the anomalous behavior, most strikingly at high temperature, is also given.

1. R. Moessner, J. E. Moore, *Topological Phases of Matter* (Cambridge University Press, 2021).
2. S. T. Bramwell, M. J. P. Gingras, Spin ice state in frustrated magnetic pyrochlore materials. *Science* **294**, 1495–1501 (2001).
3. C. Castelnovo, R. Moessner, S. Sondhi, Spin ice, fractionalization, and topological order. *Annu. Rev. Condens. Matter Phys.* **3**, 35–55 (2012).
4. C. Castelnovo, R. Moessner, S. L. Sondhi, Magnetic monopoles in spin ice. *Nature* **451**, 42–45 (2008).
5. J. Snyder, J. S. Slusky, R. J. Cava, P. Schiffer, How 'spin ice' freezes. *Nature* **413**, 48–51 (2001).
6. K. Matsuhira et al., Spin dynamics at very low temperature in spin ice Dy$_2$Ti$_2$O$_7$. *J. Phys. Soc. Jpn.* **80**, 123711 (2011).
7. H. Revell et al., Evidence of impurity and boundary effects on magnetic monopole dynamics in spin ice. *Nat. Phys.* **9**, 34–37 (2013).
8. D. Pomaranski et al., Absence of Pauling's residual entropy in thermally equilibrated Dy$_2$Ti$_2$O$_7$. *Nat. Phys.* **9**, 353–356 (2013).
9. I. Ryzhkin, Magnetic relaxation in rare-earth oxide pyrochlores. *J. Exp. Theor. Phys.* **101**, 481–486 (2005).
10. L. D. Jaubert, P. C. Holdsworth, Signature of magnetic monopole and Dirac string dynamics in spin ice. *Nat. Phys.* **5**, 258 (2009).
11. L. D. C. Jaubert, P. C. W. Holdsworth, Magnetic monopole dynamics in spin ice. *J. Phys. Condens. Matter* **23**, 164222 (2011).
12. B. Tomasello, C. Castelnovo, R. Moessner, J. Quintanilla, Single-ion anisotropy and magnetic field response in the spin-ice materials Ho$_2$Ti$_2$O$_7$ and Dy$_2$Ti$_2$O$_7$. *Phys. Rev. B Condens. Matter Mater. Phys.* **92**, 155120 (2015).
13. L. Yaraskavitch et al., Spin dynamics in the frozen state of the dipolar spin ice material Dy$_2$Ti$_2$O$_7$. *Phys. Rev. B Condens. Matter Mater. Phys.* **85**, 020410 (2012).
14. G. Sala et al., Vacancy defects and monopole dynamics in oxygen-deficient pyrochlores. *Nat. Mater.* **13**, 488–493 (2014).
15. C. Paulsen et al., Far-from-equilibrium monopole dynamics in spin ice. *Nat. Phys.* **10**, 135 (2014).
16. C. Paulsen et al., Experimental signature of the attractive coulomb force between positive and negative magnetic monopoles in spin ice. *Nat. Phys.* **12**, 661 (2016).
17. C. Paulsen et al., Nuclear spin assisted quantum tunnelling of magnetic monopoles in spin ice. *Nat. Commun.* **10**, 1–8 (2019).
18. R. Dusad et al., Magnetic monopole noise. *Nature* **571**, 234–239 (2019).
19. K. Matsuhira, Y. Hinatsu, T. Sakakibara, Novel dynamical magnetic properties in the spin ice compound Dy$_2$Ti$_2$O$_7$. *J. Phys. Condens. Matter* **13**, L737 (2001).
20. K. Matsuhira et al., Slow dynamics of Dy pyrochlore oxides Dy2Sn2O7 and Dy2Ir2O7. *J. Phys. Conf. Ser.* **320**, 012050 (2011).
21. E. R. Kassner et al., Supercooled spin liquid state in the frustrated pyrochlore Dy$_2$Ti$_2$O$_7$. *Proc. Natl. Acad. Sci. U.S.A.* **112**, 8549–8554 (2015).
22. A. M. Samarakoon et al., Machine-learning-assisted insight into spin ice Dy$_2$Ti$_2$O$_7$. *Nat. Commun.* **11**, 892 (2020).
23. J. Snyder et al., Low-temperature spin freezing in the Dy$_2$Ti$_2$O$_7$ spin ice. *Phys. Rev. B Condens. Matter Mater. Phys.* **69**, 064414 (2004).
24. J. Quilliam, L. Yaraskavitch, H. Dabkowska, B. Gaulin, J. Kycia, Dynamics of the magnetic susceptibility deep in the coulomb phase of the dipolar spin ice material Ho$_2$Ti$_2$O$_7$. *Phys. Rev. B Condens. Matter Mater. Phys.* **83**, 094424 (2011).
25. M. Orendáč et al., Magnetocaloric study of spin relaxation in dipolar spin ice Dy$_2$Ti$_2$O$_7$. *Phys. Rev. B Condens. Matter Mater. Phys.* **75**, 104425 (2007).
26. D. Slobinsky et al., Unconventional magnetization processes and thermal runaway in spin-ice Dy$_2$Ti$_2$O$_7$. *Phys. Rev. Lett.* **105**, 267205 (2010).
27. V. Kaiser, S. T. Bramwell, P. C. Holdsworth, R. Moessner, ac Wien effect in spin ice, manifest in nonlinear, nonequilibrium susceptibility. *Phys. Rev. Lett.* **115**, 037201 (2015).
28. S. R. Giblin, S. T. Bramwell, P. C. Holdsworth, D. Prabhakaran, I. Terry, Creation and measurement of long-lived magnetic monopole currents in spin ice. *Nat. Phys.* **7**, 252–258 (2011).
29. S. V. Isakov, R. Moessner, S. L. Sondhi, Why spin ice obeys the ice rules. *Phys. Rev. Lett.* **95**, 217201 (2005).
30. P. Chandra, P. Coleman, I. Ritchey, The anisotropic kagome antiferromagnet: A topological spin glass? *J. Phys. I* **3**, 591–610 (1993).
31. A. Samarakoon et al., Aging, memory, and nonhierarchical energy landscape of spin jam. *Proc. Natl. Acad. Sci. U.S.A.* **113**, 11806–11810 (2016).
32. T. Bilitewski, M. E. Zhitomirsky, R. Moessner, Jammed spin liquid in the bond-disordered kagome antiferromagnet. *Phys. Rev. Lett.* **119**, 247201 (2017).
33. T. Bilitewski, R. Moessner, Disordered flat bands on the Kagome lattice. *Phys. Rev. B* **98**, 235109 (2018).
34. J. G. Rau, M. J. Gingras, Spin slush in an extended spin ice model. *Nat. Commun.* **7**, 1–7 (2016).
35. M. Goryca et al., Field-induced magnetic monopole plasma in artificial spin ice. *Phys. Rev. X* **11**, 011042 (2021).
36. M. Ruminy, S. Chi, S. Calder, T. Fennell, Phonon-mediated spin-flipping mechanism in the spin ices dy$_2$ti$_2$o$_7$ and ho$_2$ti$_2$o$_7$. *Phys. Rev. B* **95**, 060414 (2017).

6 of 6 | **PNAS**
https://doi.org/10.1073/pnas.2117453119

Samarakoon et al.
Anomalous magnetic noise in an imperfectly flat landscape
in the topological magnet Dy$_2$Ti$_2$O$_7$